Spontaneous Thermal Waves in a Magnetized Plasma

D. C. Pace,* M. Shi, J. E. Maggs, G. J. Morales, and T. A. Carter

Department of Physics and Astronomy, University of California, Los Angeles, Los Angeles, California 90095, USA

(Received 4 March 2008; published 18 July 2008)

Coherent temperature oscillations corresponding to thermal (diffusion) waves are observed to be spontaneously excited in a narrow temperature filament embedded in a large, but colder, magnetized plasma. The parallel and transverse propagation properties of the waves satisfy the predictions of the classical transport theory based on Coulomb collisions. The frequency of the oscillations meets the conditions for a quarter-wave thermal resonator. This is the plasma version of thermal resonators used in the study of other states of matter.

DOI: 10.1103/PhysRevLett.101.035003 PACS numbers: 52.20.Fs, 52.25.Fi, 52.25.Kn, 52.35.Lv

In recent years the venerable topic of thermal (diffusion) waves [1] has received increased attention [2], primarily in the context of modern methodologies for diagnosing the properties of condensed and gaseous matter. Advances in experimental techniques and in the understanding of the mathematical properties of diffusion equations driven by sinusoidally, time-varying sources have resulted in the concept of thermal-wave resonators [3]. The frequency dependence of driven resonators is currently used to measure the properties of liquids [4], gases [5], and liquid-gas mixtures [6]. Although thermal waves have not been as extensively studied in the plasma state [7,8], some of their features have been effectively used to deduce subtle issues of the anomalous cross-field transport in tokamak devices [9,10]. A complexity of thermal waves in magnetized plasmas is that the thermal conductivity along the magnetic field, $\kappa_\parallel$, is several orders of magnitude larger than across, $\kappa_\perp$. In addition, the numerical value of $\kappa_\parallel$ can be quite large. This makes the study of thermal waves in plasmas considerably more difficult than in the undergraduate ''Angstrom modulation'' experiment [11]. The plasma systems must accommodate a long, and spatially isolated, heated region whose length along the magnetic field is much larger than the cross-field dimension. Such a situation is reported in this Letter. By injecting a weak electron beam into a large, cold, magnetized plasma, a hot electron filament is established whose length is a thousand times larger than its cross-field extent [12,13]. This configuration provides an environment akin to the thermal resonators developed for other states of matter, but, in addition, the free energy available is found to spontaneously generate a highly coherent thermal resonant cavity mode.

The parallel and transverse complex wave numbers of a thermal wave at frequency ω can be obtained by linearizing the equation describing diffusive heat transport in a uniform magnetized plasma [14] as done by Angström [1] for a scalar medium. The results are

$$k_\parallel = (1+i)\sqrt{\frac{3\omega n}{4\kappa_\parallel}}, \qquad k_\perp = (1+i)\sqrt{\frac{3\omega n}{4\kappa_\perp}}. \tag{1}$$

For a plasma whose transport is determined by Coulomb collisions [14,15] the electron thermal conductivities are given by, $\kappa_\parallel = 3.16 n T_e \tau_e / m$, $\kappa_\perp = 1.47 \kappa_\parallel (\Omega_e \tau_e)^{-2}$ with the electron collision time being $\tau_e = 3.44 \times 10^5 T_e^{3/2}/(n\lambda)$. Here, n is the plasma density, T_e is the electron temperature (in eV), m is the electron mass, Ω_e is the electron gyrofrequency, and λ is the Coulomb logarithm. If the parallel and transverse phase velocities, or the axial and radial damping coefficients, of a thermal wave can be measured, the values of the corresponding conductivities can be obtained. Furthermore, the ratio of the real (or imaginary) parts of the radial and axial wave numbers yields a measurement of the electron collision time, as shown later.

The experiment is performed in the upgraded large plasma device (LAPD-U) [16] operated by the Basic Plasma Science Facility (BaPSF) at the University of California, Los Angeles. A pulsed helium plasma column, 70 cm in diameter and 18 m long, with density in the range of $1\text{–}3 \times 10^{12}$ cm^{-3}, is used. The results reported are obtained for a magnetic field strength of 900–1000 G. The plasma pulses are repeated at a 1 Hz rate with a high degree of reproducibility. The experiment consists of injecting a small electron beam into the afterglow phase of the plasma, 0.5 ms after the main discharge voltage pulse is terminated. In the afterglow the background plasma density is still high, but the plasma temperature is low. During the main discharge $T_e = 6\text{–}8$ eV, but at the time of beam injection it has cooled to about 2 eV due to electron heat loss by conduction to the ends of the device. During the main discharge the ion temperature remains below 1 eV. In the afterglow it equilibrates with T_e, while the plasma density decays on a slow time scale of about 2 ms due to ambipolar flow to the ends of the device.

The electron beam is produced by heating a 3 mm diameter single crystal of lanthanum-hexaboride and biasing it 20 V relative to the mesh anode of the source, resulting in a peak current of 250 mA. The beam is injected at plasma center in the direction towards the cathode of the device, 16 m away. For the low beam voltage used, the

extra ionization produced by the beam electrons is negligible. The beam electrons are slowed down by the background plasma and deposit their energy in a distance of approximately 1 m from the injection point. The beam therefore produces a heat source a few millimeters in diameter and about a meter in length. Heat conduction parallel to the magnetic field results in a hot channel approximately nine meters in length and five millimeters in radial extent, with peak T_e of about 6 eV. Thus the system approximates a nearly ideal situation consisting of a temperature filament embedded in an infinite, colder plasma. This is the environment in which the thermal waves are explored.

The electron temperature is obtained as a continuous function of time from I-V traces reconstituted from an ensemble of Langmuir probe measurements. The individual members of the ensemble are obtained by measuring the current, I, drawn by a small, planar, probe whose bias voltage, V, is held constant during a single discharge but is incrementally changed after 20 discharge pulses have been recorded at that voltage. In this manner a statistical I-V curve is constructed from which the value of T_e can be deduced at any time by a suitable exponential fit [17]. This technique uses 2000, nearly identical, plasma discharges. Such an approach is required because the probe characteristic cannot be swept sufficiently fast over the desired range to measure wave properties within a single pulse. The advantage of the technique is that it permits the study of changes in T_e with high temporal and spatial resolution.

The existence of a spontaneous thermal oscillation (i.e., not externally excited by an oscillatory source) is shown in Fig. 1. It displays the time evolution of T_e at an axial position $z = 224$ cm from the beam injector and a radial location corresponding to the filament center. Figure 1(a) shows the time development over the full beam-pulse (10 ms). It exhibits a spontaneously generated oscillation superimposed on the nearly steady-state temperature of the filament. Figure 1(b) is an enlarged view over a 2.2 ms range that highlights the coherency of the oscillation. The solid curves are experimental measurements and the dashed curves are the predictions of a two-dimensional, time-dependent transport code that uses classical thermal conductivities based on Coulomb collisions. The details of the transport code have been previously described in Sec. IV of Ref. [13]. The effective heating source is modeled as a uniform cylinder 1 m in length (the beam thermalization length) and radius equal to that of the beam crystal. The error bar in Fig. 1(a) (seen at 6 ms) represents the standard deviation of the entire statistical ensemble used to obtain T_e. The code result in Fig. 1(a) does not model the thermal wave, while in Fig. 1(b) an oscillatory heat source is included whose radial extent is $1/3$ that of the unperturbed beam. Its frequency is 5.1 kHz and its amplitude corresponds to 50% of the heat deposited by the unperturbed beam. The bottom trace in Fig. 1(a) shows the time variation of the injected beam current. It indicates that current modulation is not the source of the thermal oscillations. A possible candidate for their origin is the analog of the heat-flux instability found in the solar wind [18] and in laser-plasma interactions [19].

The nonoscillatory time evolution of the electron temperature is described to a high level of precision by classical transport theory as demonstrated in Fig. 1(a). This is a nontrivial result because the phenomena involves simultaneous axial and radial heat transport over a range where the nonlinear dependence of $\kappa_\parallel$ and $\kappa_\perp$ is sampled. It is also evident from the comparison in Fig. 1(b) that a model based on a thermal wave that propagates radially and axially according to classical transport is in quantitative agreement with the observations. It should be noted that, to a large extent, the apparent temporal damping seen in the thermal oscillation in Fig. 1(a) is due to a loss of shot-to-

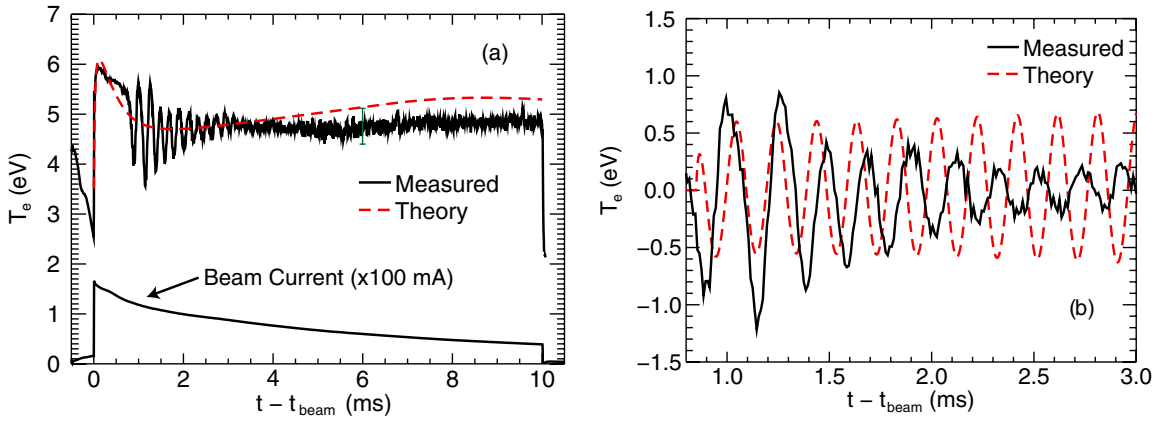

FIG. 1 (color online). Time evolution of electron temperature, T_e, at a position 224 cm axially away from the beam source at the filament center. (a) Development over the full beam-pulse. (b) The spontaneous coherent thermal oscillation over a 2.2 ms interval. Solid curves are experimental measurements and dashed curves are predictions of the transport code. The code result in (a) does not include a driven thermal wave, while in (b) a modulation at 5.1 kHz is included. The bottom trace in (a) is the injected beam current.

shot coherency in the ensemble of the 2000 independent discharge pulses. The thermal oscillations are apparently phase locked to the turn-on of the beam pulse, but this phase locking has a degree of variability which leads to the apparent temporal damping. The ion saturation current ($I_{sat} \propto \sqrt{T_e}$) for an individual pulse contains oscillations extending over time intervals much longer than indicated in Fig. 1(a).

The axial propagation of the thermal wave is measured using a cross-spectral technique. Two Langmuir probes are placed $\Delta z = 384$ cm apart axially. One of these is fixed at approximately $r = 0.15$ cm to ensure that low frequency oscillations related to the thermal wave are detected while also minimizing perturbations during a full two-dimensional cross-field scan performed by the other probe. The phase difference (cross phase) between the measured signals as a function of frequency and position is extracted from the cross-spectrum and used to compute the axial phase velocity at the frequency of the thermal wave [20]. No filtering of the raw time signals is necessary in this procedure. The minimum phase difference found in the measurement plane is used to obtain a lower bound on the parallel phase velocity (i.e., an upper bound on the real part of the parallel wave number). The measured axial phase velocity of the thermal oscillation extracted from this technique is $v_{\|} = 1.9 \times 10^7$ cm/sec, in good agreement with the value predicted by the transport code, $v_{\|} = 2.2 \times 10^7$ cm/sec.

As expected from (1), the relatively large value of the imaginary part of the transverse wave number, due to the low transverse thermal conductivity, should result in strong radial localization of the thermal oscillations. Such behavior is demonstrated in Fig. 2, where it is seen that the thermal fluctuations have a much smaller radial extent

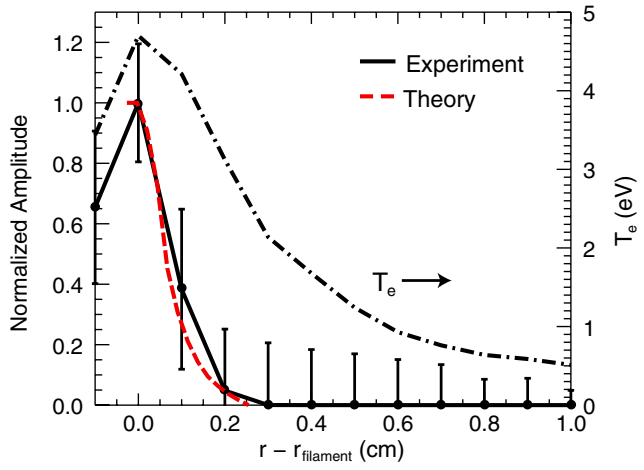

FIG. 2 (color online). Solid curve shows the radial dependence of the normalized amplitude of the coherent thermal oscillations at $z = 544$ cm. Dashed curve is the prediction of the transport code. The top dashed-dotted curve is the radial profile of the electron temperature filament.

than the region heated by the beam. The radial decay rate of the fluctuation amplitude can be estimated from the observed radial profile of the fluctuations. The spatial shape of the thermal radiation pattern is determined by the convolution of the thermal wave Green's function and the source of the thermal oscillations. For a delta function source, the radial decay of the radiation amplitude will be determined by the imaginary part of the transverse wave number, $A(r) = A_0 \exp(-r/\delta_r)$, where the decay length δ_r is the inverse of the imaginary part of the transverse wave number ($\delta_r = 1/\mathrm{Im}(k_\perp)$). For a source with finite radial extent, convolution will result in a slower radial decay in the radial amplitude. Thus, the measured decay rate of the fluctuation amplitude can provide an upper bound on the decay length and thus a lower bound on the imaginary part of the transverse wave number. In Fig. 2 the solid curve is the measured radial dependence of the amplitude of the thermal oscillations (integrated over the frequency range 3.7–6 kHz) and the dashed curve is the prediction of the transport code. Again, good agreement is obtained. From these curves the radial damping length can be extracted. The extracted value is $\delta_r = 0.10$ cm while the code predicts 0.09 cm. The top curve in Fig. 2 is the nonoscillatory electron temperature profile. It is much broader than the radial pattern of the thermal oscillation.

From measurements of the decay rate of the radial profile of the fluctuation amplitudes and the axial phase velocity of the thermal wave, the ratio of the imaginary part of the transverse wave number to the real part of the parallel wave number, the quantity $\mathrm{Im}(k_\perp)/\mathrm{Re}(k_\|)$, can be estimated. Using Eq. (1), this ratio is $\mathrm{Im}(k_\perp)/\mathrm{Re}(k_\|) = (\kappa_\|/\kappa_\perp)^{1/2} = \Omega_e \tau_e/1.21$, which yields a value of the collision time, $\tau_e = 5.93 \times 10^{-7}$ s. This value can be compared to a direct evaluation for nominal parameters ($T_e = 5$ eV, $n = 10^{12}$ cm^{-3}, $\lambda = 10$) of $\tau_e = 3.87 \times 10^{-7}$ s. Given the spatial variations of the parameters and intrinsic experimental uncertainties, these values are consistent.

The transport code can be used further to understand the origin of the oscillation frequency displayed by the coherent thermal wave, as is illustrated by the axial dependence shown in Fig. 3. The solid black curve labeled T_e is the calculated steady-state axial temperature profile; it exhibits an overall length of about 8–9 m. The horizontal solid red line corresponds to a phase value of $\pi/2$. The remaining two curves are labeled within the legend of the figure. The solid blue line (code) is the phase of the thermal mode predicted by the transport code while the dashed green line (WKB) is the Wentzel-Kramers-Brillouin phase determined from (1) for the calculated profile. The intersection of the horizontal red line with the phase curves indicates the axial position corresponding to one-quarter wavelength. Indeed, it is seen that the temperature filament behaves as a quarter-wave resonator for the thermal oscillation. An independent estimate of the length, L, of the

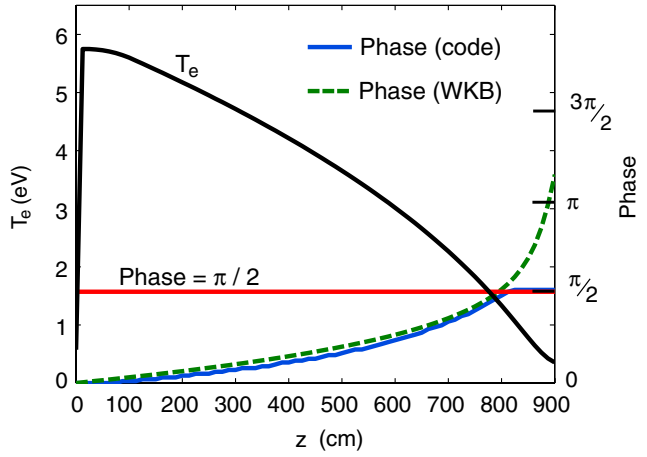

FIG. 3 (color online). Axial dependence of resonator. Curve labeled T_e is the steady-state axial temperature profile predicted by transport code. Solid blue curve is the axial phase of a temperature wave at 5.1 kHz also obtained from the code. Dashed green line is a WKB phase calculation using the dispersion relation of Eq. (1). Red line corresponds to a wave phase of $\pi/2$. Intercept of curves shows system behaves as a quarter-wave thermal resonator.

resonator can be deduced from the measured axial phase velocity based on the following relationship deduced from Eq. (1),

$$f_R = \frac{\pi \kappa_\parallel}{6L^2 n}, \tag{2}$$

in which f_R is the thermal-wave frequency. This yields $L = 9.4$ m.

From a closer examination of Fig. 1(b) it can be seen that there is a relative slippage between the calculated thermal wave, of constant frequency, and the measured signal. This implies that the spontaneously excited mode undergoes small frequency shifts as the parameters of the effective quarter-wave resonator evolve in time. The frequency extrema are 3.9 and 5.2 kHz, though the higher frequencies are achieved within approximately 0.5 ms of the initial oscillations. Experimental determination of the frequency change in time is achieved by manually measuring the period of the thermal oscillation for the distinct periods observed.

Although the detailed mechanism that triggers the spontaneous oscillations requires further investigation, the results show that a temperature filament embedded in a colder, magnetized plasma supports coherent thermal oscillations. These correspond to diffusion waves that satisfy the quarter-wave resonator condition along the magnetic field. The radial and axial properties of this resonator mode are consistent with the classical theory of transport based on Coulomb collisions. These results suggest that specially designed, oscillatory electron beam sources could use this phenomenon to explore anomalous transport behavior in magnetized plasmas. Also, it is possible that similar oscillations may be encountered in natural environments leading to filamentary structures, e.g., the solar corona.

D. C. P. and T. A. C. acknowledge support from NSF CAREER Grant No. PHY-0547572 and DOE Fusion Science Center Cooperative Agreement No. DE-FC02-04ER54785. J. E. M. and G. J. M's work performed under the auspices of the BaPSF, which is jointly supported by a DOE-NSF cooperative agreement.

*pace@physics.ucla.edu

[1] A. J. Angström, Ann. Phys. (Berlin) **190**, 513 (1862).
[2] A. Mandelis, Phys. Today **53**, 29 (2000).
[3] J. Shen and A. Mandelis, Rev. Sci. Instrum. **66**, 4999 (1995).
[4] J. A. Balderas-López, A. Mandelis, and J. A. Garcia, Rev. Sci. Instrum. **71**, 2933 (2000).
[5] M. Bertolotti, G. L. Liakhou, R. L. Voti, S. Paoloni, and C. Sibilia, Int. J. Thermophys. **19**, 603 (1998).
[6] B. Z. Azmi, H. S. Liaw, and Z. Abbas, Rev. Sci. Instrum. **76**, 074901 (2005).
[7] K. W. Gentle, Phys. Fluids **31**, 1105 (1988).
[8] A. Jacchia, P. Mantica, F. D. Luca, and G. Gorini, Phys. Fluids B **3**, 3033 (1991).
[9] P. Mantica, D. V. Eester, X. Garbet, F. Imbeaux, L. Laborde, M. Mantsinen, A. Marinoni, D. Mazon, D. Moreau, N. Hawkes *et al.*, Phys. Rev. Lett. **96**, 095002 (2006).
[10] A. Casati *et al.* (JET EFDA contributors), Phys. Plasmas **14**, 092303 (2007).
[11] H. C. Bryant, Am. J. Phys. **31**, 325 (1963).
[12] A. T. Burke, J. E. Maggs, and G. J. Morales, Phys. Rev. Lett. **81**, 3659 (1998).
[13] A. T. Burke, J. E. Maggs, and G. J. Morales, Phys. Plasmas **7**, 544 (2000).
[14] S. I. Braginskii, in *Reviews of Plasma Physics*, edited by M. A. Leontovich (Consultants Bureau, New York, 1965), Vol. 1, p. 205.
[15] L. Spitzer and R. Härm, Phys. Rev. **89**, 977 (1953).
[16] W. Gekelman, H. Pfister, Z. Lucky, J. Bamber, D. Leneman, and J. Maggs, Rev. Sci. Instrum. **62**, 2875 (1991).
[17] I. H. Hutchinson, *Principles of Plasma Diagnostics* (Cambridge University Press, Cambridge, 2002), p. 71, 2nd ed.
[18] D. W. Forslund, J. Geophys. Res. **75**, 17 (1970).
[19] V. T. Tikhonchuk, W. Rozmus, V. Y. Bychenkov, C. E. Capjack, and E. Epperlein, Phys. Plasmas **2**, 4169 (1995).
[20] J. S. Bendat and A. G. Piersol, *Random Data: Analysis and Measurement Procedures* (Wiley-Interscience, New York, 2000), p. 148, 3rd ed.